MAGI-2 scaffold protein is critical for kidney barrier function

Minna D. Balbas[a,1], Michael R. Burgess[b,1], Rajmohan Murali[c,d], John Wongvipat[a], Brian J. Skaggs[e], Peter Mundel[f], Astrid Weins[g], and Charles L. Sawyers[a,h,2]

[a]Human Oncology and Pathogenesis Program, [c]Department of Pathology, [d]Marie-Josée and Henry R. Kravis Center for Molecular Oncology, and [h]Howard Hughes Medical Institute, Memorial Sloan–Kettering Cancer Center, New York, NY 10065; [b]Division of Hematology and Oncology, Department of Medicine, University of California, San Francisco, CA 94143; [e]Division of Rheumatology, Department of Medicine, David Geffen School of Medicine, University of California, Los Angeles, CA 90095; [f]Department of Medicine, Harvard Medical School, Massachusetts General Hospital, Boston, MA 02114; and [g]Department of Pathology, Harvard Medical School, Brigham and Women's Hospital, Boston, MA 02115

Contributed by Charles L. Sawyers, September 10, 2014 (sent for review July 10, 2014; reviewed by Börje Haraldsson and Jeffery B. Hodgin)

MAGUK Inverted 2 (MAGI-2) is a PTEN-interacting scaffold protein implicated in cancer on the basis of rare, recurrent genomic translocations and deletions in various tumors. In the renal glomerulus, MAGI-2 is exclusively expressed in podocytes, specialized cells forming part of the glomerular filter, where it interacts with the slit diaphragm protein nephrin. To further explore MAGI-2 function, we generated *Magi-2*–KO mice through homologous recombination by targeting an exon common to all three alternative splice variants. *Magi-2* null mice presented with progressive proteinuria as early as 2 wk postnatally, which coincided with loss of nephrin expression in the glomeruli. *Magi-2*–null kidneys revealed diffuse podocyte foot process effacement and focal podocyte hypertrophy by 3 wk of age, as well as progressive podocyte loss. By 5.5 wk, coinciding with a near-complete loss of podocytes, *Magi-2*–null mice developed diffuse glomerular extracapillary epithelial cell proliferations, and died of renal failure by 3 mo of age. As confirmed by immunohistochemical analysis, the proliferative cell populations in glomerular lesions were exclusively composed of activated parietal epithelial cells (PECs). Our results reveal that MAGI-2 is required for the integrity of the kidney filter and podocyte survival. Moreover, we demonstrate that PECs can be activated to form glomerular lesions resembling a noninflammatory glomerulopathy with extensive extracapillary proliferation, sometimes resembling crescents, following rapid and severe podocyte loss.

MAGI-2/S-SCAM | glomerulosclerosis

MAGI-2 is a member of the membrane-associated guanylate kinase (MAGUK) family of scaffolding proteins. MAGUK proteins share a common basic domain structure, consisting of PDZ domains (named for MAGUK proteins: PSD-95, Dlg, and ZO-1), a Src homology (SH3) domain or a WW motif (two conserved tryptophan containing motifs), and a catalytically inactive guanylate kinase-like (GUK) domain. Through these protein–protein interaction domains, MAGUK proteins function as molecular scaffolds to coordinate signaling complexes (1–4). The MAGI subfamily of MAGUK proteins (MAGI 1–3) contain these same protein domains, but in the reverse orientation (MAGUK Inverted). Both MAGI-1 and MAGI-3 proteins have a relatively ubiquitous expression pattern, and localize to epithelial tight junctions (5–7). There are three protein isoforms of MAGI-2 (previously known as AIP1/S-SCAM/ARIP1), derived from alternative splicing and different initiation ATG methionines (8, 9).

MAGI-2 is highly expressed in mouse brain at synaptic junctions (10, 11), and in glomerular podocytes of the kidney (12). MAGI-2 was also identified in a multiprotein complex in rat kidney glomeruli, where it interacts with nephrin (13), a transmembrane signaling receptor and essential component of the slit diaphragm, a specialized cell–cell junction that prevents urinary protein loss (14, 15). The filtration barrier of the kidney is a highly specialized structure, composed of glomerular endothelial cells, glomerular basement membrane, and interdigitating podocyte foot processes bridged by the slit diaphragm protein complex (16). The integrity of this barrier to maintain ultrafiltration of plasma depends on the proper expression and signaling of the components of the slit diaphragm (16–18). Several mutations in the gene that encodes nephrin (*NPHS1*), and other components of the slit diaphragm complex, have been described in patients with congenital nephrotic syndrome (14, 19).

We previously identified MAGI-2 as a PTEN-interacting protein, and found that this interaction stabilizes PTEN expression and enhances its tumor-suppressor activity (20). More recent deep sequencing studies have found translocations involving *MAGI-2* and *PTEN* in human prostate tumors (21), and genetic deletion and rearrangement of *MAGI-2* in a human melanoma cell line (22). *MAGI-2* has also been identified as a target of miRNAs that are upregulated in tumors (23, 24), and is hypermethylated in cervical cancer tissue (25).

To study the in vivo role of MAGI-2, we generated mice with germ-line inactivation of *Magi-2*. Here, we show that mice with homozygous germ-line *Magi-2* inactivation are viable and born at expected Mendelian ratios. However, they present with early-onset, progressive proteinuria and severe noninflammatory, proliferative glomerulopathy with collapsing and crescent-like features within

Significance

MAGUK Inverted 2 (MAGI-2) is a scaffold protein with a putative tumor-suppressor role and also interacts with nephrin in the glomerular slit diaphragm protein complex. To gain insight into its function, we generated *Magi-2*–KO mice and found that loss of MAGI-2 expression leads to slit diaphragm disruption, podocyte foot process effacement, and severe podocyte loss. *Magi-2*–null mice develop rapidly progressive glomerular disease and renal failure. Our findings suggest that MAGI-2 is essential for kidney filter function and podocyte survival, thereby providing insights into the pathogenesis of proteinuric kidney disease. Moreover, *Magi-2*–null mice can serve as an excellent model system for studying glomerular disease progression and identification of new treatment targets for the difficult-to-treat spectrum of primary podocytopathies.

Author contributions: M.D.B., M.R.B., P.M., A.W., and C.L.S. designed research; M.D.B., M.R.B., J.W., and A.W. performed research; B.J.S., P.M., and A.W. contributed new reagents/analytic tools; M.D.B., M.R.B., R.M., P.M., A.W., and C.L.S. analyzed data; and M.D.B., P.M., A.W., and C.L.S. wrote the paper.

Reviewers: B.H., University of Gothenburg; and J.B.H., University of Michigan.

The authors declare no conflict of interest.

Freely available online through the PNAS open access option.

Data deposition: The data reported in this paper have been deposited in the Mouse Genome Database, www.informatics.jax.org (accession no. MGI:5508897).

[1]M.D.B. and M.R.B. contributed equally to this work.

[2]To whom correspondence should be addressed. Email: sawyersc@mskcc.org.

This article contains supporting information online at www.pnas.org/lookup/suppl/doi:10.1073/pnas.1417297111/-/DCSupplemental.

a few weeks after birth. The onset of glomerular dysfunction in *Magi-2*$^{\Delta/\Delta}$ mice coincides with a decrease in protein abundance of nephrin and increase in protein abundance of CIN85, an adaptor protein that regulates turnover of the slit diaphragm complex (26). Ultrastructural analysis of glomeruli from MAGI-2–null mice revealed diffuse podocyte injury, followed by rapid and severe podocyte loss and decline in kidney function, resulting in death from renal failure by 3 mo of age. Our data support an essential role for MAGI-2 in the maintenance of the kidney filter by promoting podocyte survival.

Results

Generation of *Magi-2*–KO Mice. We disrupted the *Magi-2* gene by homologous recombination in 129 LW1 ES cells by replacing a genomic fragment of exon 4 (*Magi-2* transcript variant 1) with a neomycin resistance cassette (Fig. 1*A*). Exon 4 encodes a portion of the GUK domain common to all three MAGI-2 protein isoforms. By using an external probe, correct targeting was confirmed in 12 of 576 G418 resistant colonies by Southern blot (Fig. 1*B*). ES cells were injected into C57BL/6 (B6) blastocysts, and resulting male chimeras were crossed with B6 or 129/SvJ (129) females. Offspring were genotyped initially by Southern blot and subsequently by PCR (Fig. 1*C*). Heterozygous *Magi-2*$^{\Delta/+}$ mice were intercrossed to generate *Magi-2*$^{\Delta/\Delta}$ mice. Germ-line transmission was achieved with two distinct ES clones (no. 94 and no. 278) that were analyzed in parallel. Both lines displayed the same phenotype, with the data presented hereafter from line 94. Western blot analysis and quantitative RT-PCR (qRT-PCR) performed on brain protein lysates and RNA from littermates of each genotype confirmed the loss of protein and mRNA transcript expression in KO mice (Fig. 1*D* and Fig. S1).

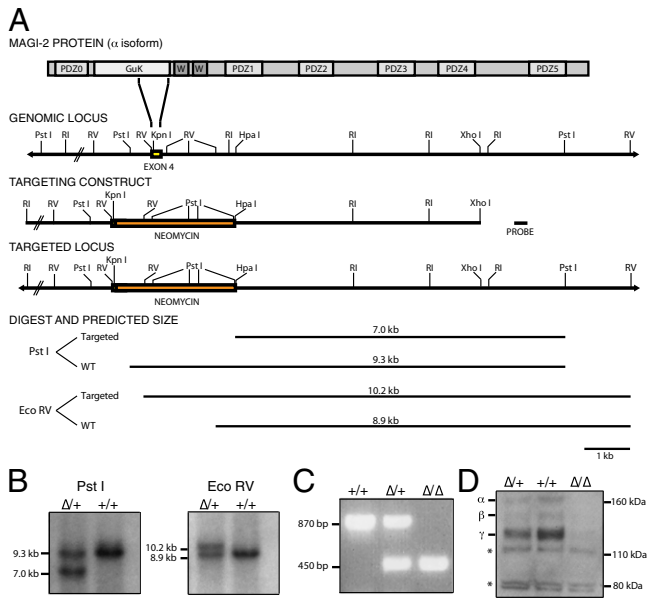

Fig. 1. Generation of *Magi-2*$^{\Delta/\Delta}$ mice. (*A*) Schematic representation for the insertion of a neomycin-resistance cassette and intragenic deletion of exon 4 of the *Magi-2* genomic locus. Restriction sites in the flanking introns and targeted exon, and the predicted sizes of fragments from PstI and EcoRV digestion are shown. The location of the 3′ probe for Southern blot analysis is also shown. (*B*) Southern blot analysis of WT ($^{+/+}$) and targeted ($^{\Delta/+}$) ES clones using the 3′ probe outside the targeting construct. (*C*) PCR genotyping of WT ($^{+/+}$), heterozygous ($^{\Delta/+}$), and KO ($^{\Delta/\Delta}$) *Magi-2* mice. (*D*) Western blot analysis of whole brain lysates from WT ($^{+/+}$), heterozygous ($^{\Delta/+}$), and KO ($^{\Delta/\Delta}$) mice using the Q antibody. (Asterisks indicate nonspecific bands.)

***Magi-2*$^{\Delta/\Delta}$ Mice Show Early-Onset Proteinuria and Impaired Survival.** *Magi-2*$^{\Delta/\Delta}$ mice appeared normal at birth and were born at expected Mendelian ratios, but growth retardation became apparent within a few weeks in mice of the 129 background. The median survival of *Magi-2*$^{\Delta/\Delta}$ mice in the 129 background was 50 d ($n = 11$), and all mice died by 3 mo of age (Fig. 2*A*). *Magi-2*$^{\Delta/\Delta}$ mice on a 129 background developed progressive proteinuria by 3 wk of age (Fig. 2*B* and Fig. S2). Serum creatinine and blood urea nitrogen (BUN) levels were elevated in proteinuric *Magi-2*$^{\Delta/\Delta}$ mice (Fig. S3), thereby confirming the development of chronic kidney disease. In contrast, in the mixed (B6/129) background, the median survival of *Magi-2*$^{\Delta/\Delta}$ mice was 169 d ($n = 41$), and many of these mice lived beyond 1 y (Fig. S4*A*). Correspondingly, urinalysis in mixed-background *Magi-2*$^{\Delta/\Delta}$ mice revealed lower-grade proteinuria with variable age of onset (Fig. S4*B*). No proteinuria or adverse survival was observed in heterozygous mice of either background (Fig. 2 and Fig. S4*A*). Because of the variability and delay in phenotype in the mixed B6/129 background *Magi-2*$^{\Delta/\Delta}$ mice, subsequent analyses were performed in 129 background mice.

Nephrin Protein Levels Are Decreased Early in *Magi-2*$^{\Delta/\Delta}$ Glomeruli. We confirmed MAGI-2 protein expression in isolated glomeruli from WT mice, and this expression was absent in glomeruli isolated from *Magi-2*$^{\Delta/\Delta}$ mice (Fig. 2 *C* and *D*). Because of its proposed role as a scaffold protein, we investigated the effect of MAGI-2 deficiency on the expression of other podocyte proteins by Western blot analysis. Interestingly, nephrin protein levels were already profoundly decreased in glomeruli from *Magi-2*$^{\Delta/\Delta}$ mice 10 d postnatally, coinciding with the onset of proteinuria (Fig. 2*C*). This finding is consistent with early down-regulation of nephrin during disassembly of the slit diaphragm in many cases of glomerular disease without genetic disruption of *NPHS1* (14). In contrast, other essential slit diaphragm-associated proteins, such as podocin (27), CD2AP (28), and α-actinin-4 (29) remained unchanged at this time point. We also investigated protein expression of the known MAGI-2 targets PTEN and pAKT(S473) (20), which showed no significant changes in *Magi-2*$^{\Delta/\Delta}$ mice within the first 18 d of life (Fig. 2*C*). These findings suggest that MAGI-2 may have a specific role in orchestrating slit diaphragm maintenance by regulating nephrin protein abundance in podocytes.

CIN85 Up-Regulation Coincides with Nephrin Reduction in *Magi-2*$^{\Delta/\Delta}$ Mice. At 3 wk of age, nephrin protein expression was almost undetectable in *Magi-2*$^{\Delta/\Delta}$ glomeruli, and we observed a reciprocal increase in protein abundance of the 70-kDa and 150–170-kDa isoforms of the adaptor protein CIN85 (30) (Fig. 2*D*). To further analyze these changes in nephrin and CIN85 expression, we performed qRT-PCR on cDNA generated from isolated glomeruli and found no significant difference in either mRNA transcript (Fig. S5), indicating posttranscriptional regulation of their expression. Previous work has demonstrated a role for CIN85 in slit diaphragm turnover in podocytes (26), and these data provide evidence that nephrin may be targeted for degradation by CIN85 in the absence of MAGI-2 expression. Of note, at 3 wk of age, a mild reduction in the abundance of podocyte proteins synaptopodin (31) and podocin was observed (Fig. 2*D*), consistent with more profound podocyte injury and/or loss.

***Magi-2*$^{\Delta/\Delta}$ Mice Develop Diffuse Podocyte Injury, Resulting in a Noninflammatory Glomerulopathy with Extracapillary Epithelial Proliferation.** To assess histologic changes in the kidneys, we killed mice of each genotype at various time points, and analyzed periodic acid–Schiff (PAS)-stained kidney sections by light microscopy. The kidneys of WT ($^{+/+}$) mice showed no morphologic abnormalities in glomeruli, tubulointerstitium, or vasculature at any age (Fig. 3*A*). As shown in Fig. 3*B*, *Magi-2*$^{\Delta/\Delta}$ kidneys displayed no light microscopic changes at 11 d of age; however, at 3 wk of age, there was a mild

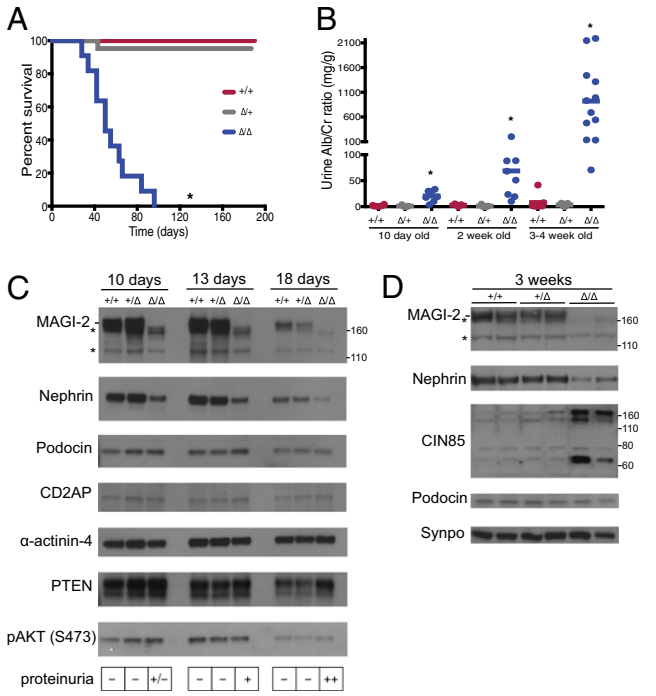

Fig. 2. *Magi-2*$^{\Delta/\Delta}$ mice show impaired survival, early proteinuria, and reduction of nephrin protein levels. (*A*) Kaplan–Meier survival curve showing significant impairment of survival of *Magi-2*$^{\Delta/\Delta}$ ($^{\Delta/\Delta}$) mice ($n = 11$) in the 129 background, compared with WT ($^{+/+}$; $n = 9$) and heterozygous ($^{+/\Delta}$; $n = 21$) littermates. The median survival for the $^{\Delta/\Delta}$ mice was 50 d, whereas $^{+/+}$ and $^{+/\Delta}$ littermates showed no impairment of their expected lifespan. (*$P < 0.001$, log-rank test). (*B*) Urinary albumin/creatinine excretion plotted for individual mice of each genotype at the indicated age. The mean from each genotype/age is shown on the graph. *Magi-2*$^{\Delta/\Delta}$ mice show a significant increase in albumin/creatinine ratio compared with WT and heterozygous littermates as early as 10 wk of age (*$P < 0.01$, Mann–Whitney test). (*C*) Western blot analysis of protein expression in glomeruli of *Magi-2*$^{+/+}$, *Magi-2*$^{+/\Delta}$, and *Magi-2*$^{\Delta/\Delta}$ mice at 10, 13, and 18 d of age. MAGI-2 expression, with a specific band expected at 170 kD, is absent in *Magi-2*$^{\Delta/\Delta}$ mice. (Asterisks indicate nonspecific bands at ∼160 and ∼120 kDa) Although nephrin expression is not different between WT and heterozygous animals, *Magi-2*$^{\Delta/\Delta}$ mice show reduction of Nephrin protein levels by 10 d postnatally, coinciding with the start of proteinuria. In contrast, other podocyte proteins, such as Podocin and CD2AP, are not altered by 18 d of age. The ubiquitous actin binding protein α-actinin-4 shows equal protein levels, and serves as loading control. PTEN and pAKT(S473), known MAGI-2 targets, are not reduced. (*D*) Western blot analysis of protein expression in glomeruli of *Magi-2*$^{+/+}$, *Magi-2*$^{+/\Delta}$, and *Magi-2*$^{\Delta/\Delta}$ mice at 3 wk of age. At 3 wk of age, Nephrin protein levels significantly reduced in all *Magi-2*$^{\Delta/\Delta}$ mice, whereas there is no difference between *Magi-2*$^{+/\Delta}$ and *Magi-2*$^{+/+}$ mice. Concurrent with the reduction of Nephrin protein, CIN85 protein expression is up-regulated in *Magi-2*$^{\Delta/\Delta}$ mice. Only a mild reduction of Podocin and Synaptopodin expression can be observed in some *Magi-2*$^{\Delta/\Delta}$ animals at 3 wk. (Asterisk indicates additional nonspecific band seen at ∼85 kD on the MAGI-2 blot.)

increase in extracellular matrix accumulation in the mesangium without glomerular hypercellularity, whereas the tubulointerstitium appeared normal. By 5.5 wk, the majority of glomeruli were severely injured, with a collapsed tuft and substantial epithelial cell proliferations (*Magi-2*$^{\Delta/\Delta}$: $49.78 \pm 10.54\%$, $n = 5$, vs. *Magi-2*$^{+/+}$: none, $n = 5$; $P = 0.0015$), in many cases resembling cellular or fibrocellular crescents (*Magi-2*$^{\Delta/\Delta}$: $15.86 \pm 3.69\%$, $n = 5$, vs. *Magi-2*$^{+/+}$: none, $n = 5$; $P = 0.0026$), notably in the absence of glomerular inflammation or hypercellularity. In keeping with the observed severe proteinuria (Fig. 2*B*), tubular protein casts were present in all *Magi-2*$^{\Delta/\Delta}$ mice. Few glomeruli were globally hyalinized (*Magi-2*$^{\Delta/\Delta}$: $4.2 \pm 1.12\%$; $n = 5$, vs. *Magi-2*$^{+/+}$: none, $n = 5$; $P = 0.0056$) or segmentally hyalinized (*Magi-2*$^{\Delta/\Delta}$: $7.44 \pm 0.69\%$; $n = 5$, vs. *Magi-2*$^{+/+}$: none, $n = 5$; $P < 0.0001$), and the tubulointerstitium showed mild tubular atrophy and interstitial fibrosis (*Magi-2*$^{\Delta/\Delta}$: $19 \pm 4\%$; $n = 5$, vs. *Magi-2*$^{+/+}$: none, $n = 5$; $P = 0.0014$). By 7 wk, the kidneys of *Magi-2*$^{\Delta/\Delta}$ mice showed widespread chronic changes of the tubulointerstitium (*Magi-2*$^{\Delta/\Delta}$: $70 \pm 10\%$; $n = 2$, vs. *Magi-2*$^{+/+}$: none, $n = 2$; $P = 0.0198$), and the vast majority of glomeruli were globally hyalinized or sclerosed (*Magi-2*$^{\Delta/\Delta}$: $59.5 \pm 15.5\%$; $n = 2$, vs. *Magi-2*$^{+/+}$: none, $n = 2$; $P = 0.0617$) with focal residual fibrous or fibrocellular extracapillary lesions (*Magi-2*$^{\Delta/\Delta}$: 7.00 ± 1.00; $n = 2$, vs. *Magi-2*$^{+/+}$: none, $n = 2$; $P = 0.0198$; Fig. 3*B* and Fig. S6).

Ultrastructural analysis by EM at 4 wk of age revealed profound podocyte injury with diffuse foot process effacement, microvillous transformation of the cell membrane, and dilation of the endoplasmic reticulum (Fig. 4). Of note, several podocytes appeared hypertrophic and showed long, thin extensions of their cell bodies. The endothelium showed mild loss of fenestrations, and the glomerular basement membrane appeared of normal thickness. Taken together, MAGI-2 deficiency causes a diffuse and progressive podocytopathy in mice.

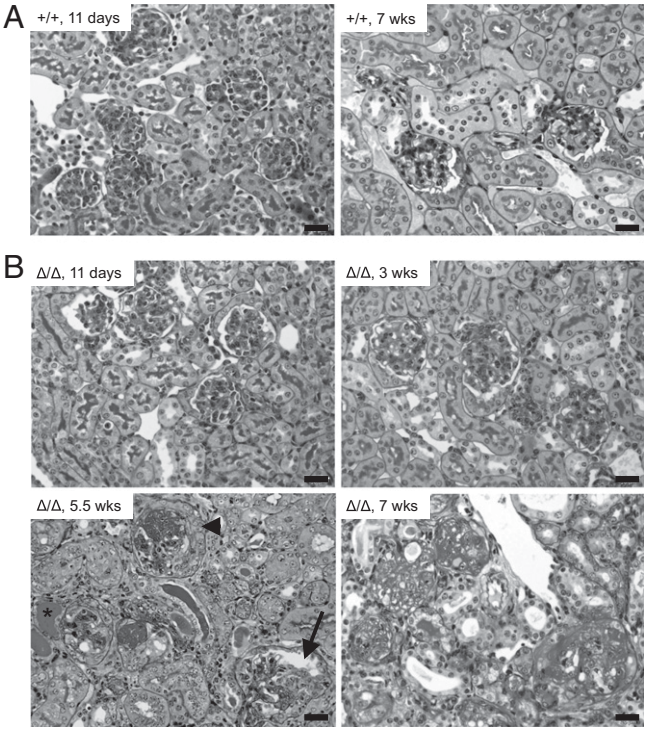

Fig. 3. *Magi-2*$^{\Delta/\Delta}$ mice develop severe and diffuse glomerular extracapillary proliferations with focal epithelial crescent formation by 5.5 wk of age. (*A*) Representative light microscopic images demonstrating morphologic changes in WT ($^{+/+}$) mice at 11 d and 7 wk of age. Glomeruli and tubulointerstitium show no significant pathologic changes (PAS staining). (Scale bars: 20 μm.) (*B*) Representative light microscopic images demonstrating morphologic changes in *Magi-2*$^{\Delta/\Delta}$ ($^{\Delta/\Delta}$) mice at 11 d, 3 wk, 5.5 wk, and 7 wk of age. At 11 d, no significant light microscopic changes are observed. At 3 wk, glomeruli show mild mesangial expansion and very focal intraglomerular cellular debris without obvious inflammation or hypercellularity, and the tubulointerstitium demonstrates no significant pathologic changes. By contrast, at 5.5 wk of age, the majority of glomeruli show segmental or global extracapillary epithelial cell proliferations and focal collapse of the tuft (arrow), resembling a severe collapsing glomerulopathy. Some proliferations resemble a cellular or fibrocellular crescent (arrowhead). Tubules contain focal protein casts (asterisk), and the interstitium shows early fibrosis with only chronic interstitial inflammation. By 7 wk, the majority of glomeruli are globally sclerosed with focal fibrous crescents, and the tubulointerstitium shows advanced chronic changes with chronic inflammation, tubular atrophy and interstitial fibrosis (PAS staining). (Scale bars: 20 μm.)

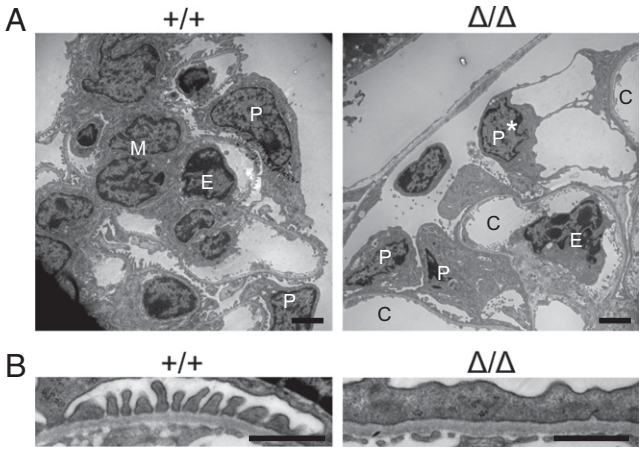

Fig. 4. *Magi-2*$^{\Delta/\Delta}$ mice show early podocyte injury. (*A*) Representative overview of ultrastructural changes in glomeruli of WT vs. *Magi-2*$^{\Delta/\Delta}$ mice at 4 wk of age. Whereas WT animals show no apparent ultrastructural changes of podocytes (marked as "P"), mesangial cells (marked as "M") and endothelium (marked as "E"), *Magi-2*$^{\Delta/\Delta}$ mice show diffuse podocyte injury, characterized by microvillous transformation and global foot process effacement. In addition, several podocytes show features of hypertrophy (asterisk), characterized by formation of long and thin cell projections, attached to glomerular capillaries (marked as "C"). (Scale bars: 2 μm.) (*B*) Magnification of foot process changes. Whereas WT mice show intact podocyte foot processes and intervening slit diaphragms lining the glomerular basement membrane, *Magi-2*$^{\Delta/\Delta}$ mice show diffuse foot process effacement with the characteristic basal actin condensation. (Scale bars: 1 μm.)

Early and Rapid Podocyte Loss in *Magi-2*$^{\Delta/\Delta}$ Mice Elicits a Proliferative Parietal Epithelial Cell Response. Podocyte loss is a hallmark of progressive proteinuric kidney disease (16). Given the development of podocyte hypertrophy and the rapid progression of kidney disease, we sought to evaluate podocyte loss as a cause of glomerular disease. We performed immunohistochemistry for the podocyte marker synaptopodin in glomeruli of WT and *Magi-2*$^{\Delta/\Delta}$ mice in various stages of disease development at 10 d, 3 wk, 5.5 wk, and 7 wk of age (Fig. 5*A*). We found that synaptopodin expression was markedly reduced in 3-wk-old *Magi-2*$^{\Delta/\Delta}$ mice compared with WT littermates, and was absent by 5.5 wk in all glomeruli with extracapillary proliferations, indicating a complete loss of podocytes (Fig. 5*B*). As progressive podocyte loss elicits a parietal epithelial cell (PEC) reaction (32), we hypothesized that the extracapillary epithelial proliferations seen in the majority of glomeruli at 5.5 wk might contain activated PECs. Immunohistochemistry for the PEC marker PAX2 confirmed that all proliferative and crescentic lesions were exclusively composed of PECs (Fig. 5*C*). The majority of PECs within those lesions were positive for KI67, indicating cell cycle activation, whereas the macrophage marker CD68 was negative (Fig. S7). These data indicate that PEC activation and proliferation represents a response to rapid and severe podocyte loss in *Magi-2*$^{\Delta/\Delta}$ mice, leading to an early-onset proliferative and noninflammatory glomerulopathy that ultimately results in death from renal failure.

Discussion

Previous reports had documented MAGI-2 expression in glomerular podocytes (12, 13), but its function in these highly specialized cells remained unknown. In this study, we present in vivo evidence that MAGI-2 is essential for kidney filter maintenance and preservation of podocytes. Mice deficient for all three MAGI-2 protein isoforms develop progressive proteinuria as a result of a severe podocytopathy, and ultimately die of renal failure. We also show that nephrin, an essential slit diaphragm protein, is reduced early in glomeruli of *Magi-2*$^{\Delta/\Delta}$ mice. Our data suggest that MAGI-2 acts as a molecular scaffold to maintain the nephrin multiprotein signaling complex.

Nephrin is commonly reduced in patients with nephrotic syndrome without a specific nephrin (i.e., *NPHS1*) mutation (15). Therefore, *Magi-2*$^{\Delta/\Delta}$ mice may serve as a clinically relevant model for slit diaphragm destruction and progressive proteinuria, in which nephrin reduction occurs before any apparent light microscopic abnormalities. Our findings suggest that loss of

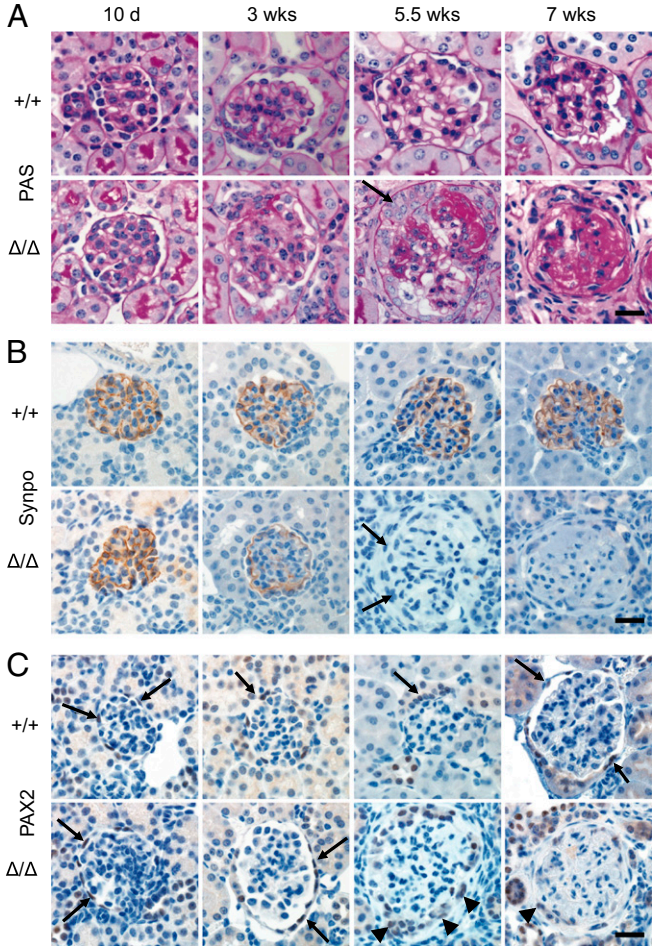

Fig. 5. Immunohistochemical analysis of glomerular changes in *Magi-2*$^{\Delta/\Delta}$ mice at 10 d, 3 wk, 5.5 wk, and 7 wk of age. (*A*) Representative light microscopic changes in glomeruli. Whereas glomeruli of WT mice show no significant light microscopic changes at any age, *Magi-2*$^{\Delta/\Delta}$ mice show a progressive glomerulopathy. At 10 d of age, no significant glomerular change is seen. At 3 wk of age, glomeruli appear mildly hypocellular compared with WT mice and show a mild increase in matrix accumulation. By 5.5 wk of age, the majority of glomeruli show a hyalinized and collapsed tuft associated with a severe extracapillary cell proliferation, in many cases resembling an epithelial cell crescent connecting the glomerulus and Bowman capsule (arrow). No significant glomerular inflammation can be seen. By 7 wk, most glomeruli are globally sclerosed with hyalinization of the tuft. (*B*) Synaptopodin (Synpo) expression in glomeruli. WT mice show preserved synaptopodin staining at all ages. At 10 d of age, no significant reduction in synaptopodin expression is seen in *Magi-2*$^{\Delta/\Delta}$ mice. As early as 3 wk of age, a mild reduction of synaptopodin can be seen, with a complete loss of synaptopodin staining in all glomeruli with extracapillary proliferations at 5.5 wk of age. Of note, epithelial cells within the proliferations are negative for synaptopodin (arrows). No synaptopodin staining is detected in globally sclerosed glomeruli. (*C*) PAX2 expression in glomeruli. WT mice show PAX2 staining limited to small, flat PEC nuclei lining Bowman capsule (arrows) at all ages. *Magi-2*$^{\Delta/\Delta}$ glomeruli show similar distribution of PAX2 at 10 d and 3 wk of age (arrows). All cells composing the extracapillary proliferations (arrowheads) are positive for PAX2 at 5.5 wk. Only occasional PAX2-positive cells are seen in globally sclerosed glomeruli at 7 wk of age. (Scale bars: 20 μm.)

nephrin is an early causative event in the development of proteinuria in *Magi-2*$^{\Delta/\Delta}$ mice. MAGI-2 has been shown to physically interact with nephrin (13, 33), raising the possibility that the interaction is required for nephrin localization or protein stability. Intriguingly, it has been previously shown that the adaptor protein CIN85 can bind to nephrin and contribute to the regulation of nephrin ubiquitination and turnover (26). Here we find an increase in CIN85 protein abundance in glomeruli of *Magi-2*$^{\Delta/\Delta}$ mice, suggesting that MAGI-2 may directly regulate CIN85-mediated nephrin turnover in podocytes. The near-complete loss of podocytes and the rapid progression of glomerular disease in *Magi-2*$^{\Delta/\Delta}$ mice are unusual and cannot be explained purely on the basis of nephrin reduction. These findings suggest an additional, nephrin-independent prosurvival role for MAGI-2 in podocytes, perhaps by blocking the proapoptotic signaling properties of dendrin (34), another MAGI-2 interacting protein (35).

Our results also provide evidence that primary podocyte injury, when severe enough, can lead to a fulminant proliferative glomerulopathy resembling a crescentic glomerulonephritis without an obvious inflammatory component. The cells composing the proliferative lesions in *Magi-2*$^{\Delta/\Delta}$ mice are PAX2-positive and synaptopodin-negative, indicating their PEC origin. A tumor suppressor function of MAGI-2 in PECs seems unlikely, as there is no documented evidence of MAGI-2 expression in this cell type. However, similar activation and proliferation of PECs, although less pronounced, was recently described in murine Adriamycin-induced nephropathy following podocyte loss (32). Thus, we attribute the observed severity of the glomerular lesions in *Magi-2*$^{\Delta/\Delta}$ mice to the particularly rapid and abundant podocyte loss, and, as such, would include a noninflammatory proliferative glomerulopathy at the extreme end of the spectrum of primary podocytopathies.

Despite high MAGI-2 expression in the adult brain, we found no evidence of morphological aberrations in the brains of *Magi-2*$^{\Delta/\Delta}$ mice. A previous study found that mice with a genetic deletion of only the α-isoform of MAGI-2/S-SCAM were born at normal Mendelian ratios but died within 24 h of birth (36). Iida et al. found no evidence of abnormal brain development or structure in the S-SCAMα–null mice, but neurons cultured from these mice displayed abnormal elongation of dendritic spines as a result of NMDA-dependent RhoA activation (36). It is of particular interest that mice lacking the α-isoform display earlier lethality than we observe in mice lacking all three isoforms, raising the possibility that each MAGI-2 isoform may have a distinct function in different tissues or that feedback regulation may occur between the different isoforms. We cannot formally exclude the possibility that strain differences also account for phenotypic differences between these mice.

Although we detected comparable pathologic and functional changes in the kidneys of *Magi-2*$^{\Delta/\Delta}$ mice on the 129 and the mixed B6/129 background, the onset of kidney disease was significantly delayed and heterogeneous in the mixed background. This is comparable to findings in several mouse models of congenital nephrotic syndrome, in which the severity of the phenotype depended on the mouse strain. For example, KO alleles of the nephrin-interacting protein podocin (i.e., *Nphs2*) develop proteinuria and glomerulosclerosis in a B6/129 mixed background and in pure 129 mice, but onset is earlier in B6/129 mice (37). Characterization of mice null for the *CD151* gene revealed strain-dependent phenotypes, with the development of severe glomerular disease in FVB strain mice, whereas B6 mice remained normal and healthy (38). Identification of genetic modifiers of renal phenotypes in different mouse strains may provide insights into genes that affect susceptibility to develop proteinuria in humans. In this context, a reduction in *MAGI-2* copy number may confer genetic susceptibility to developing a podocytopathy following a triggering event or to a more rapid clinical progression.

We had previously identified MAGI-2 an interacting partner of the tumor suppressor PTEN, and presented data that MAGI-2 stabilizes PTEN protein expression, enhancing its phosphatase activity and tumor-suppressive function (20). Nephrin can also interact with the p85 subunit of PI3K and stimulate Akt signaling in cultured podocytes (39). We found no evidence of loss of PTEN protein stability or significant change in levels of phosphorylated Akt in the glomeruli of *Magi-2*–null mice (Fig. 2*C*), suggesting that aberrant PI3K/PTEN signaling is unlikely to account for the observed phenotype. Further studies of potential MAGI-2 tumor suppressor function will require the generation of conditional alleles to avoid early death from renal failure. In conclusion, our results reveal that MAGI-2 in podocytes is required to prevent podocyte injury and progressive kidney disease and renal failure.

Materials and Methods

***Magi-2*$^{tm1Key/+}$ Mice.** *Magi-2*$^{tm1Key/+}$ mice were generated and genotyped as described in *SI Materials and Methods*. Mice were bred and maintained at the animal facilities at the University of California, Los Angeles, or Memorial Sloan–Kettering Cancer Center. All studies were approved by the institutional animal care and use committee at both universities. *SI Materials and Methods* provides detailed protocols of isolation of glomeruli, histology, immunohistochemistry, and transmission electron microscopy.

Antibodies, Western Blot, and qRT-PCR Analysis. Antibodies for MAGI-2 were generated in rabbits as described in *SI Materials and Methods*. Additional antibodies used were as follows: α-actinin-4 (B11; Santa Cruz Biotechnology), nephrin (N2028-50; US Biological), CD2AP (B-4; Santa Cruz Biotechnology), CIN85 (H-300; Santa Cruz Biotechnology), synaptopodin (N-14; Santa Cruz Biotechnology), Neph1 (H-150; Santa Cruz Biotechnology), PTEN (A2B1; Santa Cruz Biotechnology), and pAkt-Ser473 (no. 9271; Cell Signaling Technologies). *SI Materials and Methods* provides details of Western blot and qRT-PCR analysis.

Urine Analysis of Proteinuria. Albumin and creatinine levels in mouse urine were measured by ELISA and the alkaline picrate method (Albuwell/Creatinine Companion; Exocell), according to the manufacturer protocol. Alternatively, urine samples (2 μL) from each mouse were mixed with SDS-sample loading buffer, incubated at 95 °C for 5 min, and resolved by 10% SDS/PAGE. The gels were stained with Coomassie brilliant blue for 30 min, destained for 4 h, and then dried onto Whatman paper by using a gel dryer.

Note Added in Proof. A similar phenotype of MAGI-2 deletion was reported by Nishimori and coworkers (40) while our manuscript was under review.

ACKNOWLEDGMENTS. We thank Dr. Marilyn Farquhar for helpful discussions during the early phases of this work; the molecular cytology core facility and colony management group at Memorial Sloan–Kettering Cancer Center for technical support; Celine Chiu for assistance with transmission electron microscopy; Drs. Hong Wu and Meisheng Jiang and the University of California, Los Angeles, transgenic facility and ES cell core for technical assistance; and Terri Woo at the Brigham and Women's Hospital renal pathology laboratory for expert technical assistance. M.R.B. is supported by Postdoctoral Fellowship PF-14-146-01-LIB from the American Cancer Society Hillcrest Committee. This work was supported by National Institutes of Health (NIH) Mentored Clinical Scientist Career Development Award K08 DK0933783 (to A.W.) and NIH Grants DK057683, DK062472, and DK091218 (to P.M.).

1. Funke L, Dakoji S, Bredt DS (2005) Membrane-associated guanylate kinases regulate adhesion and plasticity at cell junctions. *Annu Rev Biochem* 74:219–245.
2. Caruana G (2002) Genetic studies define MAGUK proteins as regulators of epithelial cell polarity. *Int J Dev Biol* 46(4):511–518.
3. Zmajkovicova K, et al. (2013) MEK1 is required for PTEN membrane recruitment, AKT regulation, and the maintenance of peripheral tolerance. *Mol Cell* 50(1):43–55.
4. Tsunoda S, et al. (1997) A multivalent PDZ-domain protein assembles signalling complexes in a G-protein-coupled cascade. *Nature* 388(6639):243–249.
5. Laura RP, Ross S, Koeppen H, Lasky LA (2002) MAGI-1: A widely expressed, alternatively spliced tight junction protein. *Exp Cell Res* 275(2):155–170.
6. Dobrosotskaya I, Guy RK, James GL (1997) MAGI-1, a membrane-associated guanylate kinase with a unique arrangement of protein-protein interaction domains. *J Biol Chem* 272(50):31589–31597.
7. Wu Y, et al. (2000) Interaction of the tumor suppressor PTEN/MMAC with a PDZ domain of MAGI3, a novel membrane-associated guanylate kinase. *J Biol Chem* 275(28): 21477–21485.

8. Hirao K, et al. (2000) Three isoforms of synaptic scaffolding molecule and their characterization. Multimerization between the isoforms and their interaction with N-methyl-D-aspartate receptors and SAP90/PSD-95-associated protein. *J Biol Chem* 275(4):2966–2972.
9. Shoji H, et al. (2000) Identification and characterization of a PDZ protein that interacts with activin type II receptors. *J Biol Chem* 275(8):5485–5492.
10. Hirao K, et al. (1998) A novel multiple PDZ domain-containing molecule interacting with N-methyl-D-aspartate receptors and neuronal cell adhesion proteins. *J Biol Chem* 273(33):21105–21110.
11. Wood JD, et al. (1998) Atrophin-1, the DRPLA gene product, interacts with two families of WW domain-containing proteins. *Mol Cell Neurosci* 11(3):149–160.
12. Ihara KI, Nishimura T, Fukuda T, Ookura T, Nishimori K (2012) Generation of Venus reporter knock-in mice revealed MAGI-2 expression patterns in adult mice. *Gene Expr Patterns* 22(3-4):95–101.
13. Lehtonen S, et al. (2005) Cell junction-associated proteins IQGAP1, MAGI-2, CASK, spectrins, and alpha-actinin are components of the nephrin multiprotein complex. *Proc Natl Acad Sci USA* 102(28):9814–9819.
14. Welsh GI, Saleem MA (2010) Nephrin-signature molecule of the glomerular podocyte? *J Pathol* 220(3):328–337.
15. Patrakka J, Tryggvason K (2007) Nephrin—a unique structural and signaling protein of the kidney filter. *Trends Mol Med* 13(9):396–403.
16. Greka A, Mundel P (2012) Cell biology and pathology of podocytes. *Annu Rev Physiol* 74:299–323.
17. Faul C, Asanuma K, Yanagida-Asanuma E, Kim K, Mundel P (2007) Actin up: Regulation of podocyte structure and function by components of the actin cytoskeleton. *Trends Cell Biol* 17(9):428–437.
18. Brinkkoetter PT, Ising C, Benzing T (2013) The role of the podocyte in albumin filtration. *Nat Rev Nephrol* 9(6):328–336.
19. Chiang CK, Inagi R (2010) Glomerular diseases: Genetic causes and future therapeutics. *Nat Rev Nephrol* 6(9):539–554.
20. Wu X, et al. (2000) Evidence for regulation of the PTEN tumor suppressor by a membrane-localized multi-PDZ domain containing scaffold protein MAGI-2. *Proc Natl Acad Sci USA* 97(8):4233–4238.
21. Berger MF, et al. (2011) The genomic complexity of primary human prostate cancer. *Nature* 470(7333):214–220.
22. Pleasance ED, et al. (2010) A comprehensive catalogue of somatic mutations from a human cancer genome. *Nature* 463(7278):191–196.
23. Sachdeva M, et al. (2011) MicroRNA-101-mediated Akt activation and estrogen-independent growth. *Oncogene* 30(7):822–831.
24. Kitamura K, et al. (2014) MiR-134/487b/655 cluster regulates TGF-β-induced epithelial-mesenchymal transition and drug resistance to gefitinib by targeting MAGI2 in lung adenocarcinoma cells. *Mol Cancer Ther* 13(2):444–453.
25. Chen YC, et al. (2014) Methylomics analysis identifies epigenetically silenced genes and implies an activation of beta-catenin signaling in cervical cancer. *Int J Cancer* 135(1):117–127.
26. Tossidou I, et al. (2010) CIN85/RukL is a novel binding partner of nephrin and podocin and mediates slit diaphragm turnover in podocytes. *J Biol Chem* 285(33):25285–25295.
27. Boute N, et al. (2000) NPHS2, encoding the glomerular protein podocin, is mutated in autosomal recessive steroid-resistant nephrotic syndrome. *Nat Genet* 24(4):349–354.
28. Shih NY, et al. (1999) Congenital nephrotic syndrome in mice lacking CD2-associated protein. *Science* 286(5438):312–315.
29. Kos CH, et al. (2003) Mice deficient in alpha-actinin-4 have severe glomerular disease. *J Clin Invest* 111(11):1683–1690.
30. Buchman VL, Luke C, Borthwick EB, Gout I, Ninkina N (2002) Organization of the mouse Ruk locus and expression of isoforms in mouse tissues. *Gene* 295(1):13–17.
31. Mundel P, et al. (1997) Synaptopodin: An actin-associated protein in telencephalic dendrites and renal podocytes. *J Cell Biol* 139(1):193–204.
32. Hakroush S, et al. (2014) Extensive podocyte loss triggers a rapid parietal epithelial cell response. *J Am Soc Nephrol* 25(5):927–938.
33. Babayeva S, Zilber Y, Torban E (2011) Planar cell polarity pathway regulates actin rearrangement, cell shape, motility, and nephrin distribution in podocytes. *Am J Physiol Renal Physiol* 300(2):F549–F560.
34. Asanuma K, Campbell KN, Kim K, Faul C, Mundel P (2007) Nuclear relocation of the nephrin and CD2AP-binding protein dendrin promotes apoptosis of podocytes. *Proc Natl Acad Sci USA* 104(24):10134–10139.
35. Deng F, Price MG, Davis CF, Mori M, Burgess DL (2006) Stargazin and other transmembrane AMPA receptor regulating proteins interact with synaptic scaffolding protein MAGI-2 in brain. *J Neurosci* 26(30):7875–7884.
36. Iida J, et al. (2007) Synaptic scaffolding molecule alpha is a scaffold to mediate N-methyl-D-aspartate receptor-dependent RhoA activation in dendrites. *Mol Cell Biol* 27(12):4388–4405.
37. Roselli S, et al. (2004) Early glomerular filtration defect and severe renal disease in podocin-deficient mice. *Mol Cell Biol* 24(2):550–560.
38. Baleato RM, Guthrie PL, Gubler MC, Ashman LK, Roselli S (2008) Deletion of CD151 results in a strain-dependent glomerular disease due to severe alterations of the glomerular basement membrane. *Am J Pathol* 173(4):927–937.
39. Huber TB, et al. (2003) Nephrin and CD2AP associate with phosphoinositide 3-OH kinase and stimulate AKT-dependent signaling. *Mol Cell Biol* 23(14):4917–4928.
40. Ihara K-I, et al. (2014) MAGI-2 is critical for the formation and maintenance of the glomerular filtration barrier in mouse kidney. *Am J Pathol* 184(10):2699–2708.